Earth and Planetary Science Letters 593 (2022) 117687

Contents lists available at ScienceDirect

Earth and Planetary Science Letters

www.elsevier.com/locate/epsl

# Dyke cooling upon intrusion: Subsequent shape change, cooling regimes and the effect of further magma input

Marco Loncar *, Herbert E. Huppert

*Institute of Theoretical Geophysics, King's College, Cambridge, CB2 1ST, United Kingdom of Great Britain and Northern Ireland*

ARTICLE INFO

*Article history:*
Received 19 February 2022
Received in revised form 8 June 2022
Accepted 17 June 2022
Available online 1 July 2022
Editor: C.M. Petrone

*Keywords:*
dyke intrusion
dyke shape change
heat-flow
thermal modelling

ABSTRACT

Upon emplacement of a dyke, the magma may crystallise immediately and block the dyke (blocking) or begin to melt the surrounding country rock prior to crystallisation (meltback). A numerical model is used to investigate the prevalence of these regimes and the change in shape (of horizontal cross-section) of the dyke's solidus and mobile melt extent (MME) isotherms. For static magma, the solidus narrows from its initial shape throughout cooling while the MME initially narrows prior to widening. Magma reinjection leads to widening of the MME after each injection, with a lesser to no response in the solidus aspect ratio. For static magma, the minimum dyke width at which meltback occurs is inversely proportional to the country rock temperature (with no meltback for country rock below specific temperatures determined by the specific magma properties). Considering reinjection allows for meltback at significantly lower country rock temperatures and a power law relationship is determined between this meltback width and the reinjection period. Injection of superheated magma gives rise to further widening of the MME during cooling with no effect on the solidus shape, as well as decreasing the country rock temperature required for meltback.



## 1. Introduction

The prevalence of dykes gives rise to their application in many geological fields. Dyke swarms resulting from extensional tectonics have been observed to produce crustal widening on the scale of hundreds of meters to several kilometers across the world: the Troodos ophiolite, Cyprus (Moores and Vine, 1971; Varga, 1991), the Siberian platform (Polyansky et al., 2017) and NW Australia (Magee and Jackson, 2020) are well studied examples. Through ridge push, these have also been hypothesised as a contributer to the movement of tectonic plates (Swedan, 2015; Hou, 2012). On smaller scales, dykes supply volcanic eruptions and control lava output from vents and their closing and opening is vital in predicting subsequent lava flow (Kervyn et al., 2009). Investigations of shape evolution have been carried out and compared to field measurements in Rum, Scotland and Helam mine, South Africa (Daniels et al., 2012). These found that observed dyke shapes are narrower at the centre and wider at the tips than those predicted from elastic models. Further study into modelling dyke shape change is therefore important in developing a better understanding of the governing processes behind magma cooling from initial intrusion.

The cooling time-frames of emplaced magma varies between orders of months and kiloyears (Pansino et al., 2019), depending predominantly upon size and initial temperature in relation to the country rock (Jaeger, 1968). There are two main regimes by which this cooling occurs, as discussed previously by Bruce and Huppert (1989). The first is meltback, in which the initially formed chilled margins and the surrounding country rock can be melted prior to full crystallisation of the magma. The second is blocking, where the body crystallises upon emplacement and blocks the flow of magma. The extent of these regimes significantly alters the shape change of the dyke during cooling as well as the rate of cooling, and in turn crystal growth at various positions within the dyke (Platten and Watterson, 1969; Henriquez and Martin, 1978). This variation in crystal growth is commonly seen in the presence of chilled margins (Huppert and Sparks, 1989; Healy et al., 2018). Although these regimes have been qualitatively discussed in the above literature, quantitative analysis of the regime prevalence has undergone limited investigation.

Cooling of the body is predominantly controlled by conductive movement of heat within the magma (Delaney, 1986). Within dykes, convective heat transfers are relatively small in contrast to processes in large magma chambers (Worster et al., 1990). Consideration of temperature variations due to conduction in magma has been studied in numerous cases to provide analytic solutions

* Corresponding author.
*E-mail address:* ml926@cam.ac.uk (M. Loncar).

https://doi.org/10.1016/j.epsl.2022.117687

(Carslaw and Jaeger, 1959) and in more general cases to yield numerical solutions (Alexiades and Solomon, 1993; Dehghan and Najafi, 2016). Advection can then be studied by considering the effects of magma reinjection or flow, as by Bruce and Huppert (1989).

This paper uses a numerical model to investigate temperature variation in a vertically emplaced dyke from an initial intrusion shape. Subsequent shape change and variation in cooling regimes are then evaluated. This is studied in the case of a single intrusion cooling without disturbance and in the case of further magma input through the remaining mobile melt. Numerical modelling of dyke cooling has been repeatedly undertaken (Delaney, 1986; Daniels et al., 2014; Petcovic and Dufek, 2005). These investigate cooling timeframes, dyke size and temperature variation in the surrounding country rock (the final case comparing these predictions to those observed in the Columbia River flood basalts). However, there is little literature investigating the dyke shape change (aspect ratio) during cooling in particular.

The theory behind heat loss from the body is detailed in *section 2* before being implemented numerically in the static case (cooling from initial emplacement) in *section 3*. *Section 4* then applies this model to produce results relating to: shape change, regime control factors and effects of periodic magma injection. All results are then discussed in *section 5* before presenting the conclusions in *section 6*.

## 2. Theoretical framework

### 2.1. General heat transfer with latent heat liberation

Heat loss $Q$ in and surrounding a dyke varies linearly with respect to the temperature $T$ (in degrees Kelvin). Including latent heat of crystallisation $L$, however, leads to a jump condition across the melting/crystallising temperature range, between the solidus and liquidus at temperatures $T_s$ and $T_l$ respectively. Density $\rho$ and heat capacity $c_p$ are assumed to be constant with temperature, and within different phases. This gives the heat profile

$$Q = \begin{cases} \rho c_p T, & T < T_s \\ \rho c_p T + L(T - T_s)/(T_l - T_s), & T_s < T < T_l \\ \rho c_p T + L, & T > T_l. \end{cases} \tag{1}$$

When applied to the heat equation, the system is therefore dictated by

$$(1 + Z)\frac{\partial T}{\partial t} = \kappa \nabla^2 T \tag{2}$$

$$Z = \begin{cases} L/[\rho c_p (T_l - T_s)], & T_s < T < T_l \\ 0, & otherwise \end{cases} \tag{3}$$

where $\kappa$ is the material's thermal diffusivity.

The thermal conductivity of magma and rock decreases with respect to increasing temperature; the extent of this relationship in certain magmatic rocks is discussed in Vosteen and Schellschmidt (2003). This variation in thermal conductivity can be of the order of a half, between the liquidus and initial country rock temperatures. The major effect of this variation is in the temperature evolution of the immediately surrounding country rock, as detailed by Nabelek et al. (2012) in the study of contact aureoles. Here the consequences of thermal conductivity variation are shown to be most notable in the cases of plutons. Heap et al. (2022) shows porosity and hydration of the surrounding rock to also be a factor affecting the thermal properties. Both of these considerations mainly affect the behaviour in the material surrounding large igneous bodies. Therefore, in this study of magma cooling and dyke shape, the thermal properties previously mentioned are assumed constant.

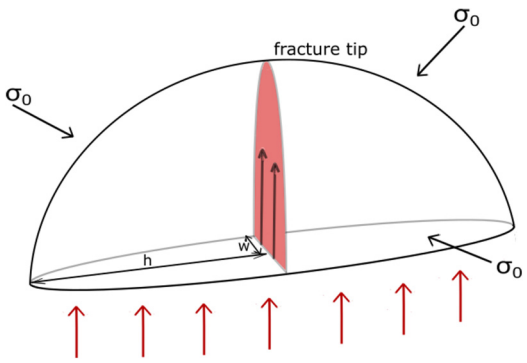


**Fig. 1.** Example of a penny shaped crack formed by the injection of fluid from a source (red arrows) along a fracture with external isotropic stress $\sigma_0$, and vertical flow shown by black arrows in the indicated cross-section. The half-width $w$ and half-length $h$ are shown with exaggerated dimensions (larger $w$ to $h$ aspect ratio than in reality). (For interpretation of the colours in the figure(s), the reader is referred to the web version of this article.)

### 2.2. Application to dyke shape

A vertical dyke can be considered as a liquid intrusion of magma that subsequently cools and crystallises. The country rock surrounding the dyke is assumed to be homogeneous and the initial shape of the dyke is governed purely by elastic laws. This shape can be approximated as the uppermost portion of a vertical penny shaped crack (Lai et al., 2015) such that the geometry is approximately linear one-dimensional (rather than radial one-dimensional). In the case of dykes, their forms are significantly narrower in one dimension than in others (*Fig. 1*). Heat loss is, therefore, predominantly in this direction - orthogonal to the plane of the dyke.

Taking a horizontal cross-section through the body gives a shape, with a vertical normal, whose perimeter is specified by

$$x = \alpha h \sqrt{1 - \frac{y^2}{h^2}}, \tag{4}$$

where $x$ and $y$ are the horizontal axes of the dyke, $h$ is the dyke half-length and $\alpha$ determines the aspect ratio of the liquid intrusion. This prefactor is determined by properties of the country rock including shear and elastic moduli as well as the surrounding hydrostatic pressure, as detailed by Lister and Kerr (1991).

It is assumed that the magma is emplaced at a single temperature $\theta_0$ in the shape detailed above, into country rock of temperature $\theta_c$. From this, a modified system to solve is obtained: *(2)* becomes the one dimensional heat equation with initial and boundary conditions,

$$(1 + Z)\frac{\partial T}{\partial T} = \kappa \frac{\partial^2 T}{\partial x^2} \tag{5}$$

$$T(x, t = 0) = \begin{cases} \theta_0, & |x| < w(y) \\ \theta_c, & |x| > w(y) \end{cases} \tag{6}$$

$$T(x \to \infty, t) = \theta_c, \tag{7}$$

where $Z$ is as stated in *(3)* and $w$ is the initial half-width of the intrusion, dependent on $y$, as specified by *(4)*. Dyke tip propagation is assumed over from the point at which cooling begins, such that the stress field during cooling is homogeneous (as shown in *Fig. 1*).

### 2.3. Inclusion of further magma input

The previous discussion concerns only the case of heat loss from a static magma, after initial emplacement. Consideration of further magma input is accomplished by treating the body of magma, at any point during cooling, as being composed of mobile and immobile sections. Immobile magma is the partially molten material that is predominantly crystallised ($\geq$ 50% partially crystallised) whilst the remaining partial melt is considered mobile (from private communication with Sparks (2021)). The mobile portion of the dyke is then able to vary in temperature in response to an assumed Newtonian flow.

The boundary temperature between mobile and immobile melt (mobile melt extent) is set to be at the midpoint between the solidus and liquidus, by assuming linear melting and crystallisation with temperature in the region of partial melt. Modification to the temperature within this central region of mobile melt is applied to represent vertical magma input [heat advection due to motion of magma in the plane is of second order in relation to heat conduction in the plane (Bartlett, 1969)]. This modification is investigated by considering periodic reinjection of magma: this causes immediate temperature change within the extent of mobile magma every time reinjection occurs. This can be seen as the temperature of the material within the mobile melt extent being raised to the liquidus temperature once every period (as specified in each figure below).

## 3. Modelling method

### 3.1. Validity of numerical model

This system of equations is known as a two-phase Stefan problem, with a range of melting/crystallisation temperatures. Although analytic solutions exist for special cases of this problem - such as in the case of a constant temperature solid and for fixed temperature static boundaries (Carslaw and Jaeger, 1959; Tao, 1978) - the system outlined in *section 2* requires a numerical approach for solution (Alexiades and Solomon, 1993). Discretisation of the $x$-domain allows for the use of a forward-step algorithm to be applied (the forward Euler method). The boundary conditions are enforced by setting the temperature at each end of the $x$-domain after every timestep. A two dimensional solution can then be found by separately calculating the time evolution following discretised line-sections along the $y$-axis.

The validity of this method is tested by applying it to a simplified temperature distribution model with known analytic solution. The simplified system chosen is that of temperature diffusion from an initial "top-hat" function *(6)* without consideration of latent heat liberation. The model is tested at discretisation levels of 50 and 200 subdivisions in the $x$-domain, with timesteps sufficiently small to ensure stability. Maximum deviations from the analytic model are 5.9% and 3.2% for the respective discretisation levels. The latter is an acceptably low error and so the method used is valid in later calculations when more than 200 subdivisions are used.

### 3.2. Application of numerical model

The previously outlined numerical method was applied to the system detailed in *section 2.2*. The position of the solidus and liquidus were chosen to agree with that of basaltic magma and country rock (Daniels et al., 2012). The initial temperature of the intrusion was set to the previously chosen liquidus to consider non-superheated magma (superheated magma is touched upon in *section 4.3*) while the initial country rock temperature was set to agree with the geotherm, with intrusion depths specified in each trial. Material properties and constant dyke parameters assumed in the computation of the following results are listed in *Table 1* [taken from Daniels et al. (2014)]. The outputs of the model are shown in *Fig. 2*, with specified differences in initial conditions, to demonstrate the resulting behaviour along a single horizontal line-section (one dimensional) through the dyke.

**Table 1**
Summary of key computational parameters and material properties used in the calculations [from Daniels et al. (2014)], assumed to be the same for the magma and host rock.

| Parameter | | Value | Unit |
|---|---|---|---|
| $\Delta x$ | Size of $x$ divisions | 0.1 | m |
| $\Delta y$ | Size of $y$ divisions | 5 | m |
| $\Delta t$ | Time step | 15770 | s |
| $h$ | Initial half-length | 1000 | m |
| $\rho$ | Density | 2800 | $\mathrm{kg\,m^{-3}}$ |
| $k$ | Thermal conductivity | 2.2 | $\mathrm{W\,m^{-1}\,K^{-1}}$ |
| $\kappa$ | Thermal diffusivity | $5.3 \times 10^{-7}$ | $\mathrm{m^2\,s^{-1}}$ |
| $L$ | Specific latent heat | $4 \times 10^5$ | $\mathrm{J\,kg^{-1}\,K^{-1}}$ |
| $c_p$ | Specific heat capacity | 1480 | $\mathrm{J\,kg^{-1}}$ |
| $T_s$ | Solidus | 950 | °C |
| $T_m$ | Mobile melt extent | 1100 | °C |
| $T_l$ | Liquidus | 1250 | °C |

To address the differences that would be observed as a result of reduced thermal conductivity (*section 2.1*), the model was also run at lower values of thermal conductivity. This shows the effects that increasing porosity and temperature of country rock would have on the behaviour of the dyke. The thermal properties used in these cases were taken from Robertson and Peck (1974), with a thermal conductivity of 1.25 $\mathrm{W\,m^{-1}\,K^{-1}}$ chosen to be appropriate. The associated results for this augmented model are given in the supplementary material.

The expected cooling regimes are observed in the testing of this model: blocking in *Fig. 2a* as the width of solidus position narrows from initially specified width; and meltback in *Fig. 2b* where the solidus position widens (minimally) before subsequent contraction. Observing these phenomena in the one dimensional solutions allows their application to be considered in *section 4*.

## 4. Results

### 4.1. Shape change

Application of the two dimensional model described in *section 3* is used to demonstrate the change in shape of a dyke, within the horizontal plane, due to initial emplacement of magma. *Fig. 3* shows the evolution of dyke shape as a temperature colour map, with isotherms of solidus and extent of mobile melt indicated. An initial half width of 10 m (aspect ratio of 0.01) is used to demonstrate the temperature profile evolution in the static magma case.

The variation in form of these isotherms is considered by calculating the aspect ratios of the solidus and extent of mobile melt at each time step. The resulting shape evolution is detailed in *Fig. 4*. Initial half-widths of 1 m and 10 m are investigated (giving initial aspect ratios of 0.001 and 0.01) along with variation in magma reinjection rate - cases with static magma and reinjection, periods of 0.15 yrs, 0.2 yrs, 3 days and 2 days as specified in the figure caption, are studied.

### 4.2. Cooling regimes

Cooling regimes of meltback and blocking, as described in *section 1*, are investigated by monitoring dyke width with respect to time. The minimum width at which meltback continues to occur is then plotted with respect to country rock temperature, as a proxy for depth. The outcome is displayed in *Fig. 5* for the case of static magma. The temperature of country rock $T$ and minimum

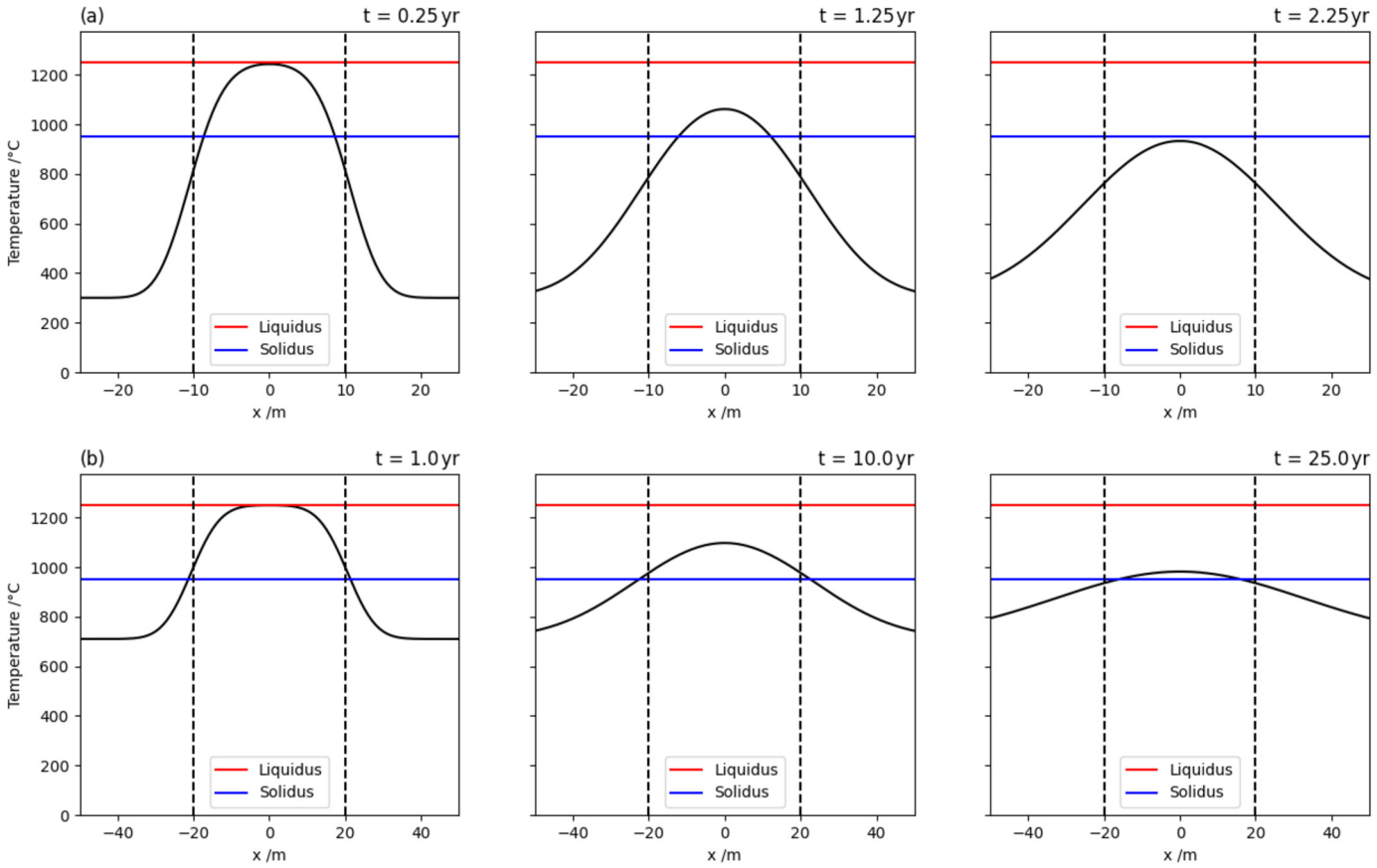


**Fig. 2.** Evolution of two temperature profiles across a line-section through a dyke demonstrating (a) blocking and (b) meltback regimes (top and bottom rows respectively), with time from intrusion specified at each step. Dotted, vertical lines represent the initial dyke width [(a) 20 m and (b) 40 m] for country rock at temperatures 300 °C and 710 °C, respectively, and solidus and liquidus isotherms are highlighted in blue and red. (For interpretation of the colours in the figure(s), the reader is referred to the web version of this article.)

half-width for meltback $w_{min}$ are seen to follow an inversely proportional relationship [$w_{min} = 93/(T - 650)$, with constants to two significant figures] as seen from the trendline with an agreement of $R^2 = 0.99$.

Magma input is then considered by altering the model as stated in *section 2.3* to observe the effects of the periodicity of magma input. *Fig. 6* shows the relationship between the minimum dyke width at which meltback occurs and the periodicity of magma input prior to analysis in *section 5.2*. These are power law trends ($w_{min} = 30P^{0.52}$ and $w_{min} = 32P^{0.50}$, with constants to two significant figures) that fit the data with $R^2$ values of 0.999 for the red and blue data sets.

### 4.3. Superheated intrusions

The previous results are related to intrusions at the liquidus; the mechanism by which the majority of dykes are formed (Daniels et al., 2014). Although rare, superheated magmas can also form intrusions. As referenced in Daniels et al. (2014), basaltic intrusions can reach 1320 °C. These magmas can also result from an impactor leading to melting of rock and subsequent layering of superheated material at temperatures up to 1700 °C (Marsh, 2013). To investigate these cases, initial intrusion temperatures of 1320 °C and 1500 °C were applied to the cases studied in *sections 4.1* and *4.2*. The results are shown in *Figs. 7* and *8*. Inversely proportional relationships are seen to produce well fitting trendlines ($R^2 = 0.998$ and 0.996 for the blue and red data sets respectively) as in *Fig. 5*. For the blue and red curves respectively, these trendlines follow $w_{min} = 200/(T - 590)$ and $w_{min} = 310/(T - 400)$, with constants to two significant figures.

## 5. Discussion

### 5.1. Observed relationships: shape change

*Fig. 3* shows that the dyke tips completely solidify significantly faster than the main body of the dyke: the temperature at the dyke tips decreases to below the solidus of the order of ten times faster than the centre of the dyke. This supports previous qualitative work (Daniels et al., 2014), which shows near immediate blocking of magma flow and crystallisation at dyke tips followed by slow cooling at dyke centres. This is accompanied by rapid cooling and solidification across the entire perimeter (more so near the minor axis than at the dyke tips), as evidenced by the immediate decreases in the aspect ratios in *Figs. 4a* and *4d*. The initial decrease from aspect ratios of 0.01 and 0.001 respectively is observed upon emplacement, showing a rapid narrowing immediately after cooling begins. This is also seen in the cases with further reinjection of magma in *Fig. 4*. This suggests that cooling of the outermost portion of the dyke is governed primarily by static magma heat diffusion.

Subsequent shape change is seen to differ between the solidus and MME isotherms. To begin with, both isotherms decrease in aspect ratio in all cases shown in *Fig. 4*, with the solidus aspect ratio continuing to decrease with time in all but *4f*. The MME isotherm decreases similarly but at lower aspect ratios. However, the MME shows an increase in aspect ratio prior to the melt becoming immobile [evidenced most in *4a* and *4d*] at which point the MME has a higher aspect ratio than the solidus. *Figs. 4b*, *4c* and *4e* show the rapid response in shape change of the MME upon reinjection: an increasing step-like pattern is seen in aspect ratios after injection. The solidus does not respond similarly, but continues to decrease,

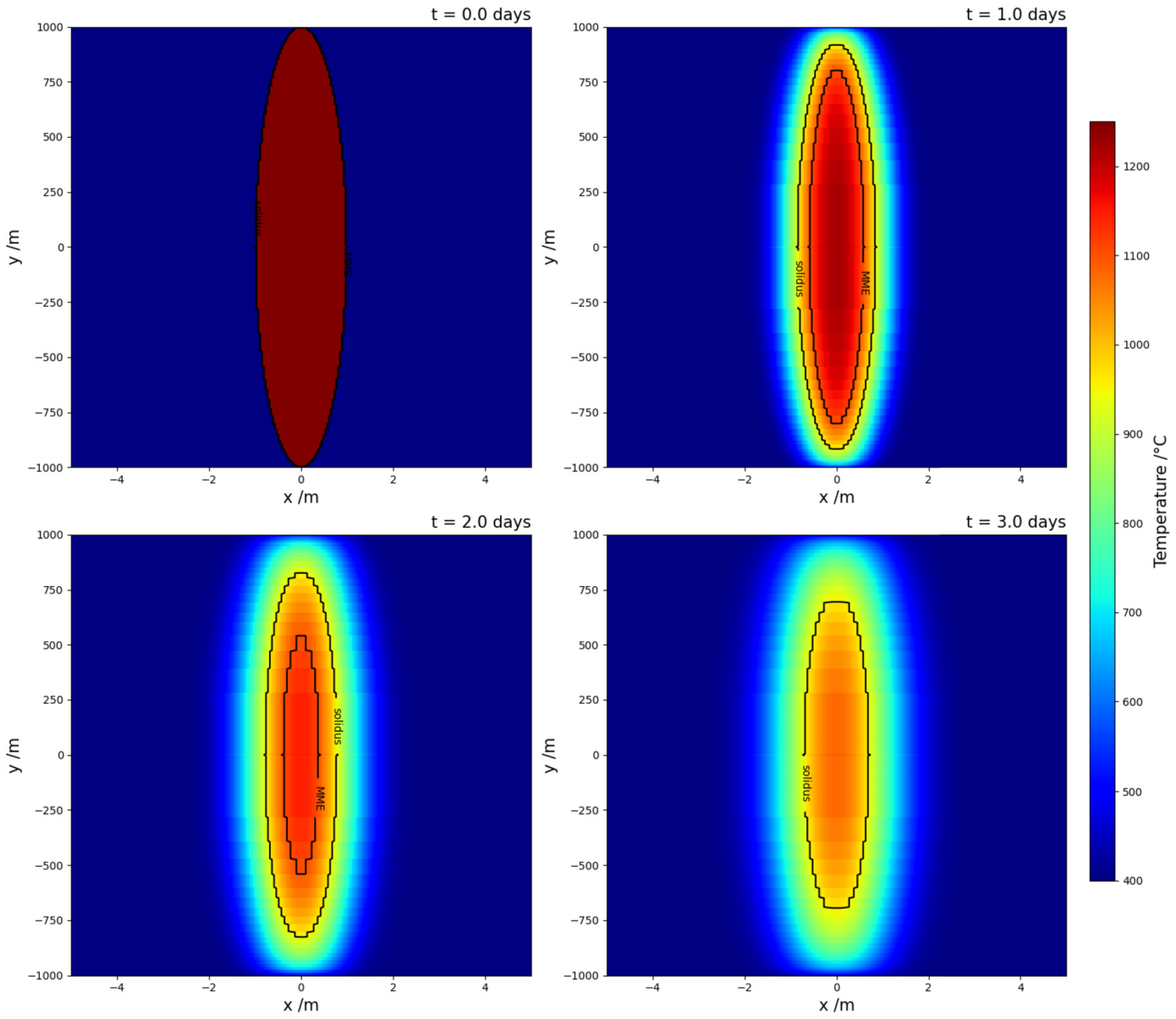


**Fig. 3.** Temperature colour plots, the evolution of the temperature profile of a dyke's horizontal cross-section, with time from initial emplacement specified at each step. Initial dyke half width of 1 m is used with a reference country rock temperature of 400 °C and the positions of the solidus and mobile melt extent (MME) isotherms are highlighted as indicated. The axes are exaggerated to demonstrate the shape change more obviously.

suggesting the effect of reinjection on shape change is primarily on the MME as opposed to the solidus. The case of significant meltback is demonstrated in *4f* where both boundaries' aspect ratios begin to increase in response to more frequent magma injection, with the MME responding earlier to the solidus. This response is near linear in both cases but with the aspect ratio of the MME increasing at a greater rate than that of the solidus (0.016 $yrs^{-1}$ compared to 0.0083 $yrs^{-1}$ in this case). However, this case involves melting of large portions of the country rock which likely have different melting characteristics to the emplaced material.

This shows that in cases of blocking, the dyke shape (solidus) narrows as it cools while the MME shape narrows before widening just prior to the partial melt becoming immobile. The MME shape is also seen to be far more responsive to magma reinjection (widening after each injection) than the solidus, which only shows this widening in the cases of significant meltback of the country rock (*Fig. 4f*). With limited reinjection, this also suggests abrupt blocking of the magma flow.

### 5.2. Observed relationships: cooling regimes

The cooling of a static body of magma is shown to be capable of producing minimal meltback of the country rock in *Fig. 2b*. *Fig. 5* shows this meltback to occur only when the surrounding country rock is at very high temperatures ($\geq 650°C$ for the chosen parameters), with a minimum temperature (indicated by a dotted line) below which it does not occur. This results in little meltback for the majority of dykes until the country rock approaches the onset of melting temperature, such as with very deep intrusions.

Consideration of reinjection produces the relationships seen in *Fig. 6*. For sufficiently long periods, the magma cools to become immobile before the subsequent reinjection and so cannot give rise to meltback; this is seen in the case of the blue points where periods greater than 0.06 years cannot be studied. The results shown for 300 °C and 400 °C country rock follow similar relationships. This suggests that dykes with half-widths of the order of 100 m or more could sustain meltback of country rock with infrequent magma reinjection based purely on conductive and latent heat

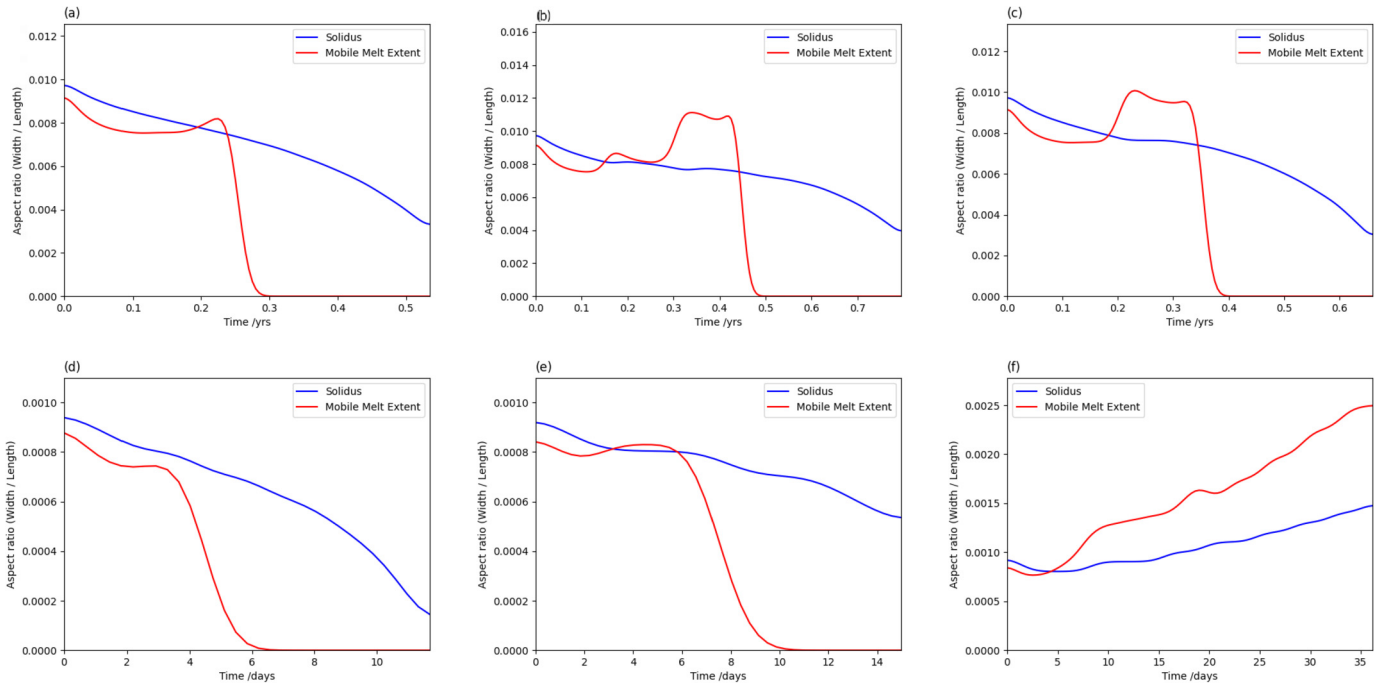


**Fig. 4.** Aspect ratio variation with time of dykes' solidus and mobile melt extent (MME) isotherms (blue and red curves respectively), in country rock at 400 °C. Initial half-widths of 10 m [(a) to (c)] and 1 m [(d) to (f)] are shown to evolve as a static mass of magma [(a) and (d)] as well as with reinjection at periods of (b) 0.15 yrs, (c) 0.2 yrs, (e) 3 days and (f) 2 days. (For interpretation of the colours in the figure(s), the reader is referred to the web version of this article.)

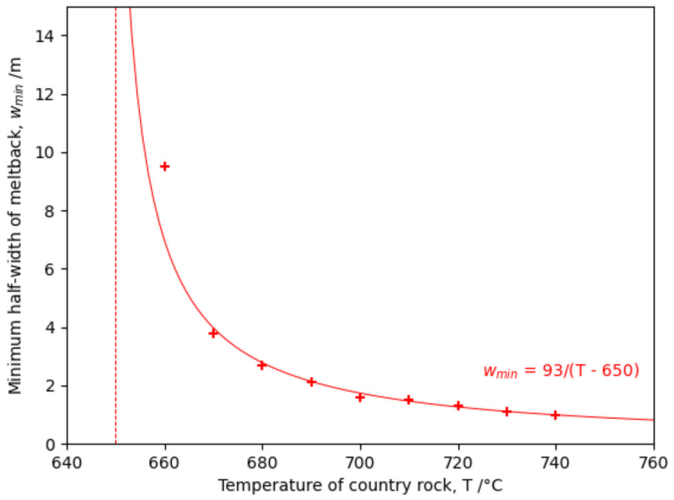


**Fig. 5.** Minimum half-width at which melting of surrounding country rock occurs as a function of the temperature of the country rock, in the case of static magma (no further input). Trendline and its are equation shown in red. (For interpretation of the colours in the figure(s), the reader is referred to the web version of this article.)

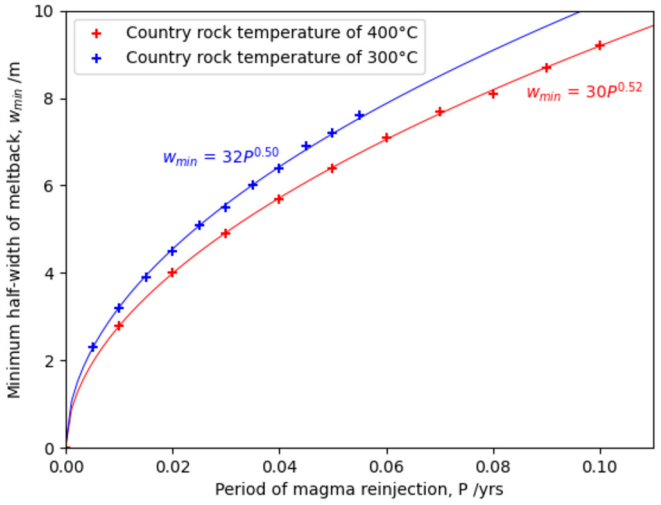


**Fig. 6.** Minimum half-width at which meltback occurs with respect to the period of magma reinjection. The relationship is shown for country rock at two different temperatures with respective trendlines and equations: 300 °C in blue and 400 °C in red. (For interpretation of the colours in the figure(s), the reader is referred to the web version of this article.)

diffusion (by extrapolation, this would only require reinjection periods of $\sim 2$ yrs).

### 5.3. Observed relationships: superheating

Comparison of the shape change between superheated intrusions and those at the liquidus is seen in *Fig. 7* (compared to *Fig. 4*). This shows the solidus isotherm to behave similarly to the non-superheated case; the aspect ratio decreases with time in both cases. The aspect ratio of the MME increases further in the superheated cases than the case in *section 5.1*. The maximum aspect ratios reached (after initial decrease) are 0.0093 and 0.0129 in *Figs. 7a* and *7b* respectively in comparison with the non-superheated case of 0.0081. This shows the more superheated the emplaced magma, the more widening of the dyke occurs during cooling.

The relationships shown in *Fig. 8* are the same as those seen in *section 5.2*, aside from the boundary temperature of country rock, below which meltback does not occur. These boundaries are found at $\geq 590$ °C and $\geq 400$ °C for the blue and red data sets respectively (parameters specified in the figure caption). The deviation from the trendline of the final three red data points likely occurs as $w_{min}$ tends to zero as temperatures approach the solidus temperature. From this it can be seen that as intrusion superheating temperature increases, the position of this boundary decreases while maintaining the same relationship between country rock temperature and minimum half-width at which meltback occurs.

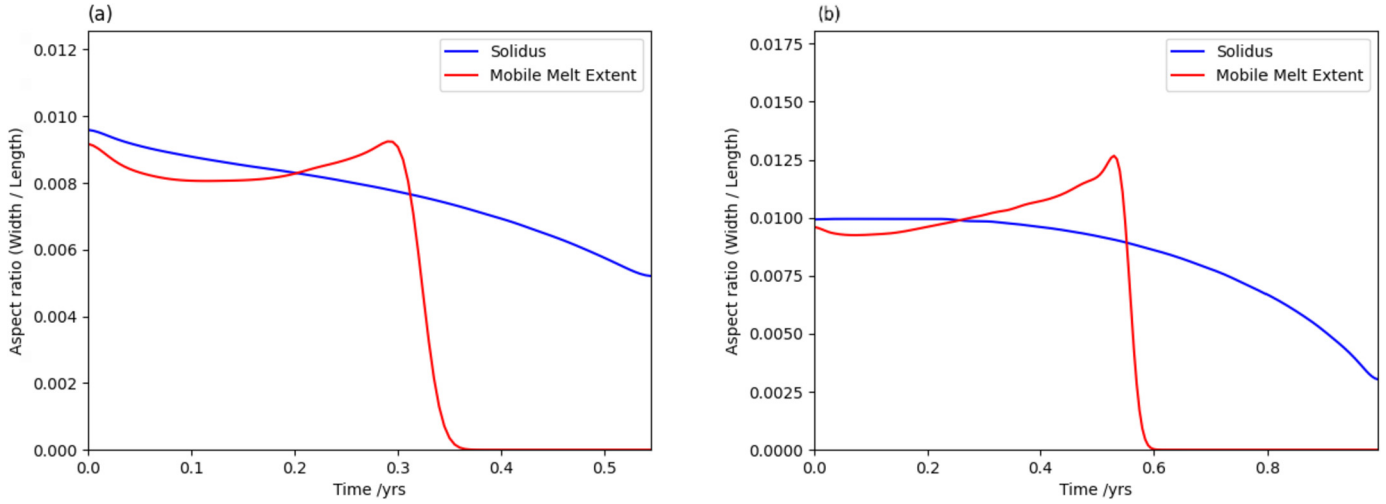


**Fig. 7.** Aspect ratio variation with time of the solidus and mobile melt extent (MME) isotherms for static cooling magma (blue and red curves respectively). The initial dyke half-width is 10 m with superheated intrusions at 1320 °C and 1500 °C, shown in (a) and (b) respectively. (For interpretation of the colours in the figure(s), the reader is referred to the web version of this article.)

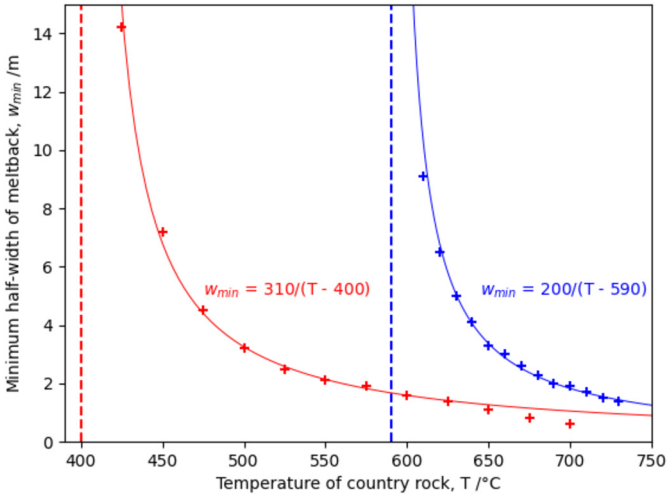


**Fig. 8.** Minimum half-width at which melting of the country rock occurs with respect to the country rock temperature in the case of static magma, for emplacement temperatures of 1320 °C and 1500 °C (blue and red respectively). Similarly coloured trendlines and equations are shown for each data set. (For interpretation of the colours in the figure(s), the reader is referred to the web version of this article.)

### 5.4. Errors and possible improvements

The main area for improvement upon this model would be to consider continuous flow, vertically through the dyke. This would occur only through the mobile melt portion of the dyke and so the information found on how the MME shape changes can be applied. The reinjection model used is also a discontinuous form of this flow and so gives rise to similar results as those found in *section 4*. Times taken for total crystallisation found with the model used are of the order of months and years (reaching the order of 10 yrs for a dyke of half-width 10 m and reinjection periods near 0.115 yrs) as opposed to the maximum kiloyears estimated in Pansino et al. (2019), likely due to this lack of flow.

Density variation of the magma with temperature is another possible area of improvement. The density of magma increases as it cools; this is of the order of $10 kgm^{-3}$ per 100 °C of cooling (Lesher and Spera, 2015). This volume change gives rise to additional stresses during cooling, which could alter the dyke shape. The effect of this change is less significant than those due to heat loss and so would likely still follow similar trends to those found here.

Another assumption that could have led to errors is that of the constant thermal properties of the magma and surrounding rock. As considered in *section 2.1*, the effects of this consideration are shown to be most prevalent in the country rock immediately surrounding the magma, particularly in the case of larger igneous bodies (Nabelek et al., 2012). In this study primarily concerning the cooling of magma (as opposed to the temperature profile in the surrounding rock), the associated errors are deemed to have little effect on dyke shape and temperature within the melt. This is seen in the supplementary material, where the dyke shape-change is seen to take the same form as in the case with lower thermal conductivity. These models run at a lower thermal conductivity are also good indicators of the behaviour of magma surrounded by a country rock with increased porosity and at a higher temperature.

The assumption of the dyke's small aspect ratio is suitable here because the dyke dimensions are consistently such that the length is much greater than the width. However, in order to apply this model to larger, non-planar igneous bodies (batholiths and magma chambers for example), two and three dimensional heat diffusion models would need to be considered. In addition, convection is not investigated here [due to its second order effects in dykes (Delaney, 1986)] but is integral in the cooling mechanisms of larger bodies (Worster et al., 1990).

### 5.5. Comparison to geological examples

The narrowing of dykes during cooling discussed in *section 5.1* suggests that dykes have thinner centres and wider tips than expected based upon initial intrusion shape. This is seen in the field where dykes are often seen to have wider tips than expected. This has been observed in the Isle of Rum, Scotland and Helam mine, South Africa by Daniels et al. (2012) and in the Jagged Rocks Complex, USA by Re et al. (2015). This is commonly attributed to interaction between dyke tips and changes in composition of the country rock. The narrowing modelled here is purely the result of the magma cooling process and so suggests that both components are important in developing this dyke shape. This also indicates that modelling dyke tip interactions and varying country rock material would be appropriate areas to build upon this study.

Rapid cooling around the dyke perimeter is shown to occur in *section 5.1*, giving rise to limited crystal development. This is particularly evident in the cases of narrow dykes with limited flow

(*Fig. 4d*). These chilled margins are commonly seen in the field, giving rise to significantly different igneous textures at dyke margins compared to their centres (Healy et al., 2018).

The meltback regimes observed in *Figs. 2b* and *4f* suggest alteration of the country rock surrounding dykes upon emplacement. This is especially prevalent in the cases with magma reinjection. Similar partial melting of the rock and alteration via contact metamorphism is seen around large dykes in the Greenland and Canada (Denyszyn et al., 2004).

Repetitive magma reinjection along the same dykes is a common method of recharge for certain volcanoes - a well studied example of which is the Krafla fissure zone in Iceland (Marquart and Jacoby, 1985). The reinjection model used here can then be applied to the evolution of dyke shapes for these such volcanoes.

## 6. Conclusion

The current investigation shows that during the cooling of magma from initial emplacement, the horizontal cross-section shape of a dyke varies from its initial form by narrowing. In all blocking regimes, the solidus isotherm narrows continuously up until crystallisation, whereas the mobile melt extent (MME) isotherm first narrows before widening, prior to the melt becoming immobile. Meltback regimes show the form of both the solidus and MME to widen (aspect ratio increasing linearly with time) but with the MME being more responsive to subsequent magma reinjection and leading the solidus shape change in time.

In addition to this, the regimes of blocking and meltback are seen to be heavily reliant on the rate of magma input. In the static magma case, meltback is very rare, occurring only in cases where the country rock is at very high temperatures (within 300 °C of the solidus) and gives rise to minimal partial melting of surrounding rock. With reinjection of magma, meltback can occur at far lower temperatures of country rock and give rise to significant partial melting. The period of reinjection and minimum dyke width for meltback are shown to follow a near linear relationship for periods of reinjection greater than 0.03 yrs.

Superheated intrusions are briefly considered and shown to increase the incidence of meltback when compared to magma emplaced at the liquidus temperature. As well as this, the greater the extent of superheating, the greater the increased widening of the MME isotherm shape during cooling, while having little to no effect on the evolution of the form of the solidus isotherm.

## CRediT authorship contribution statement

**Marco Loncar:** Formal analysis, Methodology, Software, Writing – original draft. **Herbert E. Huppert:** Conceptualization, Supervision, Writing – review & editing.

## Declaration of competing interest

The authors declare that they have no known competing financial interests or personal relationships that could have appeared to influence the work reported in this paper.

## Acknowledgements

We thank R.S.J. Sparks for his valuable geological insights and E.J. Hinch for all his stimulating help in developing the numerical models used. We also thank the Gatsby Foundation for offering support for this project to be carried out. The grant given by the Gatsby foundation was supplied via the King's College charity number 1139422. For thought provoking conversations, amusement and advice we thank A. Cox, M.-S. Liu, M. Roach, J. Saville and O.S. Wilson.

## Appendix A. Supplementary material

Supplementary material related to this article can be found online at https://doi.org/10.1016/j.epsl.2022.117687.

## References

Alexiades, V., Solomon, A.D., 1993. Mathematical Modeling of Melting and Freezing Processes. Taylor and Francis.

Bartlett, R.W., 1969. Magma convection, temperature distribution, and differentiation. Am. J. Sci. 267 (9), 1067–1082. https://doi.org/10.2475/ajs.267.9.1067.

Bruce, P., Huppert, H.E., 1989. Thermal control of basaltic fissure eruptions. Nature 342, 665–667. https://doi.org/10.1038/342665a0.

Carslaw, H.S., Jaeger, J.C., 1959. Conduction of Heat in Solids. Clarendon Press, Oxford.

Daniels, K.A., Kavanagh, J., Menand, T., Sparks, R.S.J., 2012. The shapes of dikes: evidence for the influence of cooling and inelastic deformation. Geol. Soc. Am. Bull. 124 (7/8), 1102–1112. https://doi.org/10.1130/B30537.1.

Daniels, K.A., Bastow, I.D., Keir, D., Sparks, R.S.J., Menand, T., 2014. Thermal models of dyke intrusion during development of continent–ocean transition. Earth Planet. Sci. Lett. 385, 145–153. https://doi.org/10.1016/j.epsl.2013.09.018.

Dehghan, M., Najafi, M., 2016. Numerical solution of a non-classical two-phase Stefan problem via radial basis function (RBF) collocation methods. Eng. Anal. Bound. Elem. 72, 111–127. https://doi.org/10.1016/j.enganabound.2016.07.015.

Delaney, P.T., 1986. Conductive Cooling of Dikes with Temperature-Dependent Thermal Properties and Heat of Crystallization. U.S. Geological Survey, Flagstaff, Arizona: U.S.A.

Denyszyn, S.W., Halls, H.C., Davis, D.W., 2004. A paleomagnetic, geochemical and U-Pb geochronological comparison of the Thule (Greenland) and Devon Island (Canada) dyke swarms and its relevance to the Nares Strait Problem. Polarforschung 74 (1–3), 63–75. http://hdl.handle.net/10013/epic.29925.d001.

Healy, D., Rizzo, R.E., Duffy, M., Farrell, N.J.C., Hole, M.J., Muirhead, D., 2018. Field evidence for the lateral emplacement of igneous dykes: implications for 3D mechanical models and the plumbing beneath fissure eruptions. Volcanica 1 (2), 85–105. https://doi.org/10.30909/vol.01.02.85105.

Heap, M.J., Jessop, D.E., Wadsworth, F.B., Rosas-Carbajal, M., Komorowski, J.-C., Gilg, H.A., Aron, N., Buscetti, M., Gential, L., Goupil, M., Masson, M., Hervieu, L., Kushnir, A.R.L., Baud, P., Carbillet, L., Ryan, A.G., Moretti, R., 2022. The thermal properties of hydrothermally altered andesites from La Soufrière de Guadeloupe (Eastern Caribbean). J. Volcanol. Geotherm. Res. (ISSN 0377-0273) 421, 107444. https://doi.org/10.1016/j.jvolgeores.2021.107444. https://www.sciencedirect.com/science/article/pii/S0377027321002730.

Henriquez, F., Martin, R.F., 1978. Crystal growth textures in magnetite flows and feeder dykes, El Laco, Chile. Can. Mineral. 16, 581–589.

Hou, G., 2012. Mechanism for three types of mafic dyke swarms. Geosci. Front. 3 (2), 217–223. https://doi.org/10.1016/j.gsf.2011.10.003.

Huppert, H.E., Sparks, R.S.J., 1989. Chilled margins in igneous rocks. Earth Planet. Sci. Lett. 92, 397–405. https://doi.org/10.1016/0012-821X(89)90063-0.

Jaeger, J.C., 1968. Cooling and solidification of igneous rocks. In: Hess, H.H., Arie, Poldervaart (Eds.), Basalts: The Poldervaart Treatise on Rocks of Basaltic Composition, vol. 2. John Wiley & Sons, New York.

Kervyn, M., Ernst, G., van Wyk de Vries, B., Mathieu, L., Jacobs, P., 2009. Volcano load control on dyke propagation and vent distribution: insights from analogue modeling. J. Geophys. Res. 114. https://doi.org/10.1029/2008JB005653.

Lai, C-Y., Zheng, Z., Dressaire, E., Wexler, J.S., Stone, H.A., 2015. Experimental study on penny-shaped fluid-driven cracks in an elastic matrix. Proc. R. Soc. A 471. https://doi.org/10.1098/rspa.2015.0255.

Lesher, C.E., Spera, F.J., 2015. The Encyclopedia of Volcanoes. chapter Thermodynamic and Transport Properties of Silicate Melts and Magma, second edition, pp. 113–141.

Lister, J.R., Kerr, R.C., 1991. Fluid-mechanical models of crack propagation and their application to magma transport in dykes. J. Geophys. Res. 96 (B6), 10049–10077. https://doi.org/10.1029/91JB00600.

Magee, C., Jackson, C.A., 2020. Seismic reflection data reveal the 3D structure of the newly discovered Exmouth Dyke Swarm, offshore NW Australia. Solid Earth 11, 579–606. https://doi.org/10.5194/se-11-579-2020.

Marquart, G., Jacoby, W., 1985. On the mechanism of magma injection and plate divergence during the Krafla Rifting Episode in NE Iceland. J. Geophys. Res. 90 (B12), 10178–10192. https://doi.org/10.1029/JB090iB12p10178.

Marsh, B.D., 2013. On some fundamentals of igneous petrology. Contrib. Mineral. Petrol. 166, 665–690. https://doi.org/10.1007/s00410-013-0892-3.

Moores, E.M., Vine, F.J., 1971. The Troodos massif, Cyprus and other ophiolites as oceanic crust: evaluation and implications. Philos. Trans. R. Soc. Lond. Ser. A, Math. Phys. Sci. 268, 443–467. https://doi.org/10.1098/rsta.1971.0006.

Nabelek, P.I., Hofmeister, A.M., Whittington, A.G., 2012. The influence of temperature-dependent thermal diffusivity on the conductive cooling rates of plutons and temperature-time paths in contact aureoles. Earth Planet. Sci. Lett. (ISSN 0012-821X) 317–318, 157–164. https://doi.org/10.1016/j.epsl.2011.11.009. https://www.sciencedirect.com/science/article/pii/S0012821X11006649.

Pansino, S., Emadzadeh, A., Taisne, B., 2019. Dike channelization and solidification: time scale controls on the geometry and placement of magma migration pathways. J. Geophys. Res., Solid Earth 124, 9580–9599. https://doi.org/10.1029/2019JB018191.

Petcovic, H.L., Dufek, J.D., 2005. Modeling magma flow and cooling in dikes: implications for emplacement of Columbia River flood basalts. J. Geophys. Res., Solid Earth 110 (B10). https://doi.org/10.1029/2004JB003432. https://agupubs.onlinelibrary.wiley.com/doi/abs/10.1029/2004JB003432.

Platten, I., Watterson, J., 1969. Oriented crystal growth in some tertiary dykes. Nature 223, 286–287. https://doi.org/10.1038/223286a0.

Polyansky, O.P., Prokopiev, A.V., Koroleva, O.V., Tomshin, M.D., Reverdatto, V.V., Selyatitsky, A.Y., Travin, A.V., Vasiliev, D.A., 2017. Temporal correlation between dyke swarms and crustal extension in the middle Palaeozoic Vilyui rift basin, Siberian platform. Lithos 282–283, 45–64. https://doi.org/10.1016/j.lithos.2017.02.020.

Re, Giuseppe, White, J.D.L., Ort, M.H., 2015. Dikes, sills, and stress-regime evolution during emplacement of the Jagged Rocks Complex, Hopi Buttes Volcanic Field, Navajo Nation, USA. J. Volcanol. Geotherm. Res. (ISSN 0377-0273) 295, 65–79. https://doi.org/10.1016/j.jvolgeores.2015.01.009. https://www.sciencedirect.com/science/article/pii/S0377027315000244.

Robertson, Eugene C., Peck, Dallas L., 1974. Thermal conductivity of vesicular basalt from Hawaii. J. Geophys. Res. (1896-1977) 79 (32), 4875–4888. https://doi.org/10.1029/JB079i032p04875. https://agupubs.onlinelibrary.wiley.com/doi/abs/10.1029/JB079i032p04875.

Sparks, R.S.J., 2021. Private communication. On 3rd Sept. 2021.

Swedan, N.H., 2015. Ridge push engine of plate tectonics. Geotectonics 49, 342–359. https://doi.org/10.1134/S0016852115040081.

Tao, L.N., 1978. The Stefan problem with arbitrary initial and boundary conditions. Q. Appl. Math. 36, 223–233. https://doi.org/10.1090/qam/508769.

Varga, R.J., 1991. Modes of extension at oceanic spreading centers: evidence from the Solea graben, Troodos ophiolite, Cyprus. J. Struct. Geol. 13 (5), 517–537. https://doi.org/10.1016/0191-8141(91)90041-G.

Vosteen, H.D., Schellschmidt, R., 2003. Influence of temperature on thermal conductivity, thermal capacity and thermal diffusivity for different types of rock. In: Heat Flow and the Structure of the Lithosphere. Phys. Chem. Earth Parts A/B/C (ISSN 1474-7065) 28 (9), 499–509. https://doi.org/10.1016/S1474-7065(03)00069-X. https://www.sciencedirect.com/science/article/pii/S147470650300069X.

Worster, M.G., Huppert, H.E., Sparks, R.S.J., 1990. Convection and crystallization in magma cooled from above. Earth Planet. Sci. Lett. 101, 78–89. https://doi.org/10.1016/0012-821X(90)90126-I.